

**Search for Supersymmetric Particles
at $130 \text{ GeV} < \sqrt{s} < 140 \text{ GeV}$ at LEP**

The L3 Collaboration

Abstract

A search for supersymmetric particles (charginos, neutralinos, sleptons and stop quarks) has been performed with data collected by the L3 detector during the November 1995 run of the LEP collider at centre of mass energies between 130 and 140 GeV with a total integrated luminosity of 5.1 pb^{-1} . We observe no signal for supersymmetric particles and we set improved exclusion limits on their production cross sections and masses.

Submitted to *Phys. Lett. B*

1 Introduction

The Standard Model [1] has been very successful in describing data concerning electroweak interactions. However, it leaves many fundamental parameters unexplained such as the electroweak mixing parameter, $\sin^2\theta_W$. The quadratic divergences of scalar masses at the one loop level and the large difference between the electroweak scale and the grand unification scale are further problems of the Standard Model.

Supersymmetry [2] addresses some of these questions. In minimal supersymmetric models for every particle the existence of a partner particle with spin differing by half a unit is predicted. Supersymmetric models require at least two Higgs doublets to generate the masses of the gauge bosons and of the fermions.

The fermionic partners of the W^\pm (gauginos) and of the H^\pm (higgsinos) mix to form mass eigenstates, the charginos $\tilde{\chi}_{1,2}^\pm$. The partners of the γ , of the Z , and of the neutral Higgs bosons mix to form four mass eigenstates, the neutralinos $\tilde{\chi}_1^0$, $\tilde{\chi}_2^0$, $\tilde{\chi}_3^0$ and $\tilde{\chi}_4^0$, in order of increasing mass. Each fermion is associated with two scalar supersymmetric particles, one for each helicity state, nearly degenerate in mass.

In the following we will make the usual assumptions that R-parity, a new quantum number which discriminates ordinary particles from supersymmetric particles, is conserved and that $\tilde{\chi}_1^0$ is the lightest supersymmetric particle (LSP). R-parity conservation implies that supersymmetric particles are always produced in pairs and always decay into non supersymmetric particles and $\tilde{\chi}_1^0$ which is stable and escapes detection due to its weakly interacting nature. Therefore a distinctive signature of supersymmetric particles is missing energy in the event.

Charginos are produced in pairs via Z/γ exchange in the s -channel and $\tilde{\nu}$ exchange in the t -channel. If the chargino is lighter than the scalar sparticles it decays via exchange of virtual W , sleptons, squarks or charged Higgs bosons into $\tilde{\chi}_1^0 f \bar{f}'$. If H^\pm and all squarks and sleptons are very massive, the decay branching ratios are the same as those of the $\tilde{\chi}_1^0 W^*$. On the other hand, if the slepton masses are significantly smaller than the squark masses and of the order of M_W , the leptonic branching ratios are enhanced. If the $\tilde{\nu}$ or $\tilde{\ell}$ are lighter than the chargino, the decay modes $\tilde{\chi}^\pm \rightarrow \tilde{\ell} \nu$ or $\tilde{\chi}^\pm \rightarrow \tilde{\ell} \nu$ dominate. The signatures of these decays would be covered by the slepton search but have not been explicitly taken into account. In what follows we assume the chargino to be lighter than the scalar sparticles. In general we have three possible kinds of final states: purely hadronic events, lepton plus hadrons events and purely leptonic events.

Pair production of neutralinos occurs through s -channel Z exchange and t -channel selectron exchange in all possible combinations kinematically allowed: $\tilde{\chi}_1^0 \tilde{\chi}_1^0$, $\tilde{\chi}_1^0 \tilde{\chi}_2^0$, $\tilde{\chi}_2^0 \tilde{\chi}_2^0$ and so on. The process $\tilde{\chi}_1^0 \tilde{\chi}_1^0$ is invisible in the detector while all others could be seen. Heavier neutralinos typically decay into $\tilde{\chi}_1^0 f \bar{f}$ through virtual Z exchange. Supersymmetric particle mediated decays may affect the decay branching ratios as indicated for the charginos. The higher order decay process $\tilde{\chi}_2^0 \rightarrow \tilde{\chi}_1^0 \gamma$ has not been considered in these searches.

Sleptons are produced in pairs through the s -channel process. Production of selectrons get contributions also from t -channel exchange of a neutralino which enhances the production cross section. Sleptons mainly decay into $\ell \tilde{\chi}_1^0$. The other possible decays into $\nu \tilde{\chi}^\pm$ have the same signatures as the charginos with more missing energy.

Due to the high mass of the top quark, stop quarks can be much lighter than all other squarks [3]. In addition the mass splitting by left-right mixing, $\tilde{t}_1 = \tilde{t}_L \cos \theta_{LR} + \tilde{t}_R \sin \theta_{LR}$, may drive the lower mass eigenstate \tilde{t}_1 to be the lightest supersymmetric charged state [4]. The stop quark pair production cross section depends on the stop mass, $m_{\tilde{t}}$, and the mixing

angle θ_{LR} . In the stop quark search the stop quark is assumed to be lighter than all other charged sparticles, in which case the dominant decay is into a $\tilde{\chi}_1^0$ and a charm quark.

Previous limits on the existence of supersymmetric particles have been obtained by all LEP I [5–7] and Tevatron experiments [8]. In this paper we present results of a search for charginos, neutralinos, sleptons and stop quarks performed at centre of mass energies between 130 and 140 GeV in e^+e^- collisions.

2 The L3 Detector

The L3 detector [9] consists of a silicon microstrip detector [10], a central tracking chamber (TEC), a high resolution electromagnetic calorimeter composed of BGO crystals, a lead-scintillator ring calorimeter at low polar angles [11] (ALR), a scintillation counter system, a uranium hadron calorimeter with proportional wire chamber readout, and an accurate muon chamber system. A forward-backward muon detection system extends the polar angle coverage of the muon chambers down to 24 degrees in the forward-backward region [12]. These detectors are installed in a 12 m diameter magnet which provides a solenoidal field of 0.5 T and an additional toroidal field of 1.2 T in the forward backward region. The luminosity is measured using BGO calorimeters preceded by silicon trackers [13] situated on each side of the detector.

3 Data Sample and Simulation

In this analysis we use the data collected by the L3 detector during the high energy run of LEP in November 1995, corresponding to an integrated luminosity of 5.07 pb^{-1} (2.75 pb^{-1} at $\sqrt{s} = 130.3 \text{ GeV}$, 2.27 pb^{-1} at $\sqrt{s} = 136.3 \text{ GeV}$ and 0.05 pb^{-1} at $\sqrt{s} = 140.2 \text{ GeV}$).

The main background processes at these centre of mass energies are:

- two photon interactions $e^+e^- \rightarrow e^+e^-\bar{f}\bar{f}$;
- Bhabha scattering and s -channel electroweak processes with $Z/\gamma^* \rightarrow \bar{f}\bar{f}$, including the ‘radiative return’ to the Z by means of the emission of a hard initial state radiation photon which may be lost in the beam pipe;
- other electroweak processes with small cross sections compared to the previous ones, namely $e^+e^- \rightarrow Z/\gamma^*Z^*/\gamma^*$, $e^+e^- \rightarrow WW^*$, $e^+e^- \rightarrow Zee$, $e^+e^- \rightarrow We\nu$.

Monte Carlo simulated events for the main background sources have been produced at the three centre of mass energies. The number of simulated events for the background is equivalent to about 10 times the statistics of the collected data. We use `PYTHIA` [14] to simulate all the backgrounds except Bhabha events, simulated with `BHAGENE` [15], $e^+e^- \rightarrow l^+l^-(\gamma)$, simulated with `KORALZ` [16], and $e^+e^- \rightarrow W^+W^-$, simulated with `KORALW` [17].

The two photon interaction process has the largest cross section and is by far the most copious source of background. We have generated these events requiring at least 5 GeV invariant mass of the two photon system. As a cross check and in order to have a more complete description of the two photon interactions we select two photon events in the data collected previously in 1995 at centre of mass energies around 91 GeV and we use these data to cross check the Monte Carlo predictions and the two photon rejection ability of the final selection. This is possible since two photon interactions are rather insensitive to the centre of mass energy.

Signal events have been generated at the three centre of mass energies with the program `SUSYGEN` [18], for masses of charginos, neutralinos and sleptons up to 68 GeV and for different masses of the lightest neutralino up to the kinematic limit ($M_{\tilde{\chi}_1^0} = M_{particle}$). For charginos, events have also been generated with the program `DFGT` [19], which takes into account the spin correlations between charginos. Stop quark events have been generated using a dedicated event generator [20], which assumes a short stop lifetime.

The response of the L3 detector is modelled with the `GEANT` [21] detector simulation program which includes the effects of energy loss, multiple scattering and showering in the detector materials and in the beam pipe. Additional time dependent detector inefficiencies are also taken into account.

The trigger efficiency has been studied in two ways. In the first one we use a full simulation of the algorithms of the level-1 energy and TEC triggers [9]. Randomly triggered events in coincidence with the beam crossing have been used to cross check all the relevant distributions. In the second method we have studied the energy, TEC, scintillator and muon triggers directly from the data taking advantage of the redundancy of the trigger. The two methods are in good agreement and we conservatively use the lowest efficiency to estimate the selection efficiency. The overall trigger efficiency for the various signals before the selection is reported later.

4 Experimental Procedure

We look for supersymmetric particles by using several independent analyses for the chargino [22, 23], neutralino [23], slepton [23, 24] and stop quark [23, 25] searches. Possible supersymmetric decay channels have been studied each making use of the appropriate topological and kinematical signatures. The main features of supersymmetric particle production are large missing transverse momentum, large missing energy and large acoplanarity angle due to the undetected neutralinos in the final states. Thus the different analyses reject the most offending two photon and $f\bar{f}\gamma$ backgrounds by demanding high missing transverse momentum and acoplanarity angle plus high missing mass and low visible energy. We find that the trigger and selection efficiency to detect a supersymmetric signal, for a given \sqrt{s} and sparticle mass close enough to the beam energy, depend mostly on the mass difference between the sparticle and the lightest neutralino ($\Delta M = M_{particle} - M_{\tilde{\chi}_1^0}$). Below a mass difference of 15 GeV, the decrease in multiplicity, visible energy and missing p_T reduces both trigger and selection efficiencies significantly. In this kinematical region the two photon interaction background becomes similar to the signal; therefore a different experimental strategy has been used for the low ΔM case ($\Delta M < 15$ GeV) and for the high ΔM .

In all the analyses efficiencies comparable to the ones described below are achieved and no signal is found. Therefore in what follows we report the results of a global analysis [23] which takes advantage of the common signature of all the signals in the search for charginos, neutralinos, sleptons and stop quarks.

5 Event Reconstruction

Hadronic events are reconstructed using information coming from all subdetectors. The energy of the event is obtained taking into account the energy deposition in the calorimeters and the momentum measured by the TEC and muon chambers.

We perform lepton and photon identification. Electromagnetic showers not matched with a charged track are identified as photons. Taus are identified as one, two or three prong isolated systems seen in the detector. Once the lepton and photon identification has been performed we assign to electrons and photons the energy measured in the BGO and to muons the momentum measured in the muon detector adding the average energy loss in the calorimeters and any contribution of collinear final state radiation measured in the BGO. Every cluster or track which has not been recognized as a photon, electron or muon is identified as a hadron. Jets are reconstructed with the LUCLUS [26] algorithm forcing the reconstruction of only two jets. Since in this search the main signature of the signal is missing energy, we monitor run by run the detector behaviour, since detector inefficiencies or noise may fake energy imbalance. By means of randomly triggered events in coincidence with the beam crossing we estimate the amount of noise present in the detector. The consequences on the signal efficiency due to these effects are small and taken into account in the systematic errors.

6 Selection

We make a selection on all possible final states using a single set of cut variables. The cut values are a-priori optimized using Monte Carlo signal and background events. The optimization procedure varies all the cuts simultaneously to maximize the signal efficiency and background rejection.

We take advantage of the missing energy signature to reduce the Bhabha scattering and s -channel electroweak processes by requiring the visible energy to be less than 90 GeV. To substantially decrease the contamination of tagged two photon interactions we additionally require that the energies measured in the active lead ring and in the luminosity monitors, which cover the polar angle range $1.5^\circ < \theta < 8^\circ$, are each less than 4 GeV. Next we apply five selections oriented to different final states. An event is accepted if it passes at least one of the following selections:

1. We look for two acoplanar leptons, not necessarily of the same flavour, with transverse imbalance due to the undetected neutralinos. The main background, coming from two photon interactions, has small transverse imbalance when the final state electrons escape in the beam pipe. One of the most useful variables is the absolute value of the projection of the total momentum of the two leptons onto the direction perpendicular to the thrust axis determined from the two leptons in the $R - \phi$ plane (E_{TT}) (if the two leptons form an angle of less than 90° , E_{TT} is defined as the total transverse momentum of the two leptons). This variable is mainly effective to discriminate the signal from the process $e^+e^- \rightarrow e^+e^-\tau^+\tau^-$, for which the transverse imbalance is larger than in other two photon interactions due to the undetected neutrinos coming from the τ decays. Figure 1 shows the distribution of E_{TT} , for the slepton signal, the data and the expected background, after all other cuts have been applied.
2. We select high multiplicity events with one isolated energetic lepton, which is the signature of chargino pair decays, where one decays leptonically and the other hadronically.
3. Purely hadronic decays of charginos, neutralinos and stops are selected by means of an inclusive selection of high multiplicity events.
4. Leptonic events for which at least one lepton fails the lepton identification are recovered by means of an inclusive selection of low multiplicity events with high visible energy.

Number of expected events from the background	
$e^+e^- \rightarrow Z/\gamma^*Z^*/\gamma^*$	0.3
$e^+e^- \rightarrow WW^*$	0.1
$e^+e^- \rightarrow We\nu$	0.1
$e^+e^- \rightarrow Zee$	0.1
$e^+e^- \rightarrow Z/\gamma^*$	0.1
Two photon interactions	0.2
Total	0.9

Table 1: Total number of expected events from the background after the final selection.

5. Events with small visible energy, namely low ΔM charginos, neutralinos, sleptons and stops are selected by an inclusive selection especially conceived.

Selections 3, 4 and 5 are based on the features of the event related to the missing energy, namely the missing momentum should point far from the beam pipe and should be isolated. In addition we require the missing momentum direction in the $R - \phi$ plane to be isolated from calorimetric energy deposits and charged tracks. One of the most important cuts is on the total transverse momentum, which is shown in Figure 2.

We optimize the a-priori search sensitivity which is related to the ratio between the average Poisson upper limit on the signal, without background subtraction, and the signal efficiency, $\sum_{n=0}^{\infty} k_n P_b(n)/\varepsilon$, where k_n is the 95% C.L. Poisson upper limit for n observed events and $P_b(n)$ is the Poisson distribution for observing n events with a background of b events (estimated from Monte Carlo) [27]. The efficiency ε is an average over all the significant signal topologies. The description of all the variables as well as the selection cuts used in the analysis are reported in detail in Reference 23.

When we apply our final selection with the optimized cuts we estimate from the MC background sample a total number of expected events of 0.9 (see Table 1), of which 0.6 are due to irreducible backgrounds such as $Z\gamma^*$ where the Z decays in a neutrino pair and the γ^* decays into $f\bar{f}$. No data events satisfy the selection criteria.

In Tables 2–5 we give the total efficiencies for the different signals. The efficiencies for stop quark detection are similar to those for hadronic final states of charginos.

7 Systematic Error Estimation

We derive the systematic uncertainty of the signal efficiency by simultaneously changing quantities like energies and angles, by an amount indicated by a comparison of data with Monte Carlo. We vary these quantities, in the reconstruction program, using normal distributions with standard deviations equal to the estimated uncertainties. We then repeat many times the reconstruction and obtain the average shift of the signal efficiency and its standard deviation. We take into account various sources of systematic error: the overall energy scale, the energy calibration of each subdetector, the jet angular resolution, and the tracking inefficiency.

As total systematic error we take the average shift, plus one standard deviation, of the signal detection efficiency obtained for many iterations of the reconstruction. This gives a relative uncertainty due to systematics, for $\tilde{\chi}^{\pm}$, $\tilde{\chi}_2^0$ and stop quark, ranging from 2.9%, for $\Delta M = 20$ GeV,

$\sqrt{s} = 136.3 \text{ GeV}$						
$M_{\tilde{\chi}^\pm} \text{ (GeV)}$	$M_{\tilde{\chi}^\pm} - M_{\tilde{\chi}_1^0} \text{ (GeV)}$	Trig. eff.	Eff.	Eff. LL	Eff. LH	Eff. HH
50	26	0.98	0.57	0.47	0.63	0.53
50	6	0.86	0.20	0.14	0.18	0.23
60	29	0.98	0.61	0.52	0.65	0.59
60	20	0.98	0.62	0.53	0.60	0.67
60	5	0.78	0.11	0.11	0.099	0.13
65	29	0.99	0.64	0.46	0.70	0.62
65	4	0.71	0.053	0.069	0.043	0.058
$\sqrt{s} = 130.3 \text{ GeV}$						
$M_{\tilde{\chi}^\pm} \text{ (GeV)}$	$M_{\tilde{\chi}^\pm} - M_{\tilde{\chi}_1^0} \text{ (GeV)}$	Trig. eff.	Eff.	Eff. LL	Eff. LH	Eff. HH
50	26	0.98	0.55	0.50	0.59	0.52
50	6	0.84	0.18	0.22	0.16	0.20
60	29	0.99	0.61	0.48	0.69	0.57
60	20	0.98	0.61	0.45	0.59	0.66
60	5	0.75	0.084	0.066	0.067	0.11
65	29	0.98	0.66	0.53	0.69	0.66
65	4	0.68	0.043	0.080	0.044	0.033

Table 2: Efficiencies, which include also the trigger efficiency, for the chargino selection at different centre of mass energies. The overall efficiency reported in the fourth column is evaluated assuming 100% decay branching ratio of $\tilde{\chi}^\pm \rightarrow \tilde{\chi}_1^0 W^*$. The efficiencies for the purely hadronic final state (HH), the lepton plus hadrons final state (LH) and the purely leptonic final state (LL) are also shown. The efficiencies for the stop quark search are very similar to those for hadronic decays of the charginos in the last column.

$\sqrt{s} = 136.3 \text{ GeV}$				
$M_{\tilde{\chi}^\pm} \text{ (GeV)}$	$M_{\tilde{\chi}_2^0} \text{ (GeV)}$	$M_{\tilde{\chi}_1^0} \text{ (GeV)}$	Trig. eff.	Eff.
62	44	21	0.92	0.46
63	38	21	0.96	0.32
65	44	24	0.89	0.46
66	38	24	0.96	0.53
67	44	28	0.92	0.48
68	36	26	0.97	0.36
$\sqrt{s} = 130.3 \text{ GeV}$				
$M_{\tilde{\chi}^\pm} \text{ (GeV)}$	$M_{\tilde{\chi}_2^0} \text{ (GeV)}$	$M_{\tilde{\chi}_1^0} \text{ (GeV)}$	Trig. eff.	Eff.
62	44	21	0.92	0.43
63	38	21	0.97	0.37
65	44	24	0.88	0.53

Table 3: Efficiencies, which include also the trigger efficiency, for the decay $\tilde{\chi}^\pm \tilde{\chi}^\mp \rightarrow \tilde{\chi}_1^0 \tilde{\chi}_2^0 X$ at different centre of mass energies.

$\sqrt{s} = 136.3 \text{ GeV}$			
$M_{\tilde{\chi}_2^0} \text{ (GeV)}$	$M_{\tilde{\chi}_2^0} - M_{\tilde{\chi}_1^0} \text{ (GeV)}$	Trig. eff.	Eff.
55	5	0.44	0.15
65	5	0.43	0.092
$\sqrt{s} = 130.3 \text{ GeV}$			
$M_{\tilde{\chi}_2^0} \text{ (GeV)}$	$M_{\tilde{\chi}_2^0} - M_{\tilde{\chi}_1^0} \text{ (GeV)}$	Trig. eff.	Eff.
40	12	0.70	0.30
55	5	0.44	0.14
56	35	0.83	0.51
60	6	0.73	0.43
61	29	0.80	0.53
65	5	0.42	0.074
69	11	0.59	0.27
74	50	0.97	0.60

Table 4: Trigger and total efficiencies for the neutralino selection at 136.3 and 130.3 GeV centre of mass energy for the process $e^+e^- \rightarrow \tilde{\chi}_1^0\tilde{\chi}_2^0 \rightarrow \tilde{\chi}_1^0\tilde{\chi}_1^0 X$.

		selectron		smuon		stau	
$M_{\tilde{l}} \text{ (GeV)}$	$M_{\tilde{l}} - M_{\tilde{\chi}_1^0} \text{ (GeV)}$	Trig. eff.	Eff.	Trig. eff.	Eff.	Trig. eff.	Eff.
50	27	1.00	0.64	0.95	0.58	0.93	0.46
50	11	0.99	0.66	0.92	0.58	0.79	0.26
55	32	1.00	0.69	0.95	0.62	0.94	0.47
55	6	0.88	0.51	0.82	0.48	0.59	0.069
60	37	1.00	0.66	0.95	0.61	0.94	0.54
60	5	0.85	0.54	0.79	0.48	0.53	0.057
65	42	0.97	0.63	0.96	0.62	0.95	0.56
65	26	0.97	0.62	0.96	0.67	0.93	0.52
65	10	0.98	0.68	0.95	0.62	0.69	0.25

Table 5: Trigger and total efficiencies for the slepton selection at 130.3 GeV centre of mass energy.

to 5.4%, for $\Delta M = 5$ GeV. For selectrons the relative uncertainty is almost constant as function of ΔM and is equal to 1.2%, while for smuons it is between 1.3% and 2.3%, and for staus between 2.3% and 5.3%. We do not assign any systematic error on the trigger efficiency due to the fact that our estimation is already very conservative. The background in the low angle detectors (ALR + luminosity monitor), not included in the simulation, is responsible for a relative loss of efficiency of $1.1 \pm 0.5\%$.

Other sources of systematic error on the number of expected events are: the error on the measured luminosity ($< 1\%$) and the statistical error on the signal efficiency ($\sim 2\%$ for charginos and $\sim 3\%$ for staus, selectrons, smuons and neutralinos). From a comparison between `SUSYGEN` and `DFGT` we estimate a theoretical error of 3% on the chargino production cross section and decay branching ratios and of less than 2% on the selection efficiencies due to the spin correlations. We assume this theoretical error of 3% also for other channels and in particular we assume this also covers the uncertainty related to the stop decay mechanism. Combining all these errors in quadrature we obtain, for all channels, a total relative systematic error on the number of expected events of typically 5%.

8 Results

The absence of any candidates in all the decay channels allows improved exclusion limits for charginos, neutralinos, sleptons and stop quarks to be determined. We evaluate limits reducing the number of expected signal events by one standard deviation of the total systematic error.

8.1 Upper limits on supersymmetric particle production cross sections

We set model independent upper limits on the production cross section for sparticles at $\sqrt{s} = 130.3$ GeV and $\sqrt{s} = 136.3$ GeV. We show in Figure 3 the 95% C.L. upper limit on the production cross section for a sparticle mass of 65 GeV at $\sqrt{s} = 130.3$ GeV and for a sparticle mass of 68 GeV at $\sqrt{s} = 136.3$ GeV as function of the mass difference between the sparticle and the lightest neutralino. For the upper limit on the cross section for a sparticle mass of 65 GeV we also use the integrated luminosity at $\sqrt{s} = 136.3$ GeV with the assumption that the cross section does not change. The upper limits on the production cross sections of lighter sparticles are very similar because the efficiency depends mainly on ΔM , but only weakly on the mass of the produced sparticles. Figure 3d shows the upper limits on the production cross section for the process $e^+e^- \rightarrow \tilde{\chi}_1^0\tilde{\chi}_2^0$ when the sum of the two neutralino masses equals the centre of mass energy. Limits are computed assuming 100% branching ratio of the scalar leptons into $\tilde{\chi}_1^0$ plus charged lepton, of the $\tilde{\chi}_2^0$ into $\tilde{\chi}_1^0 Z^*$ and of the stop quark into $\tilde{\chi}_1^0 c$.

8.2 Interpretation in the MSSM

In the Minimal Supersymmetric Standard Model (MSSM) [28], the Lagrangian at the unification scale is globally supersymmetric, except for a set of soft breaking mass terms. Among these are the gaugino masses M_1 , M_2 and M_3 associated with the $U(1)_Y$, $SU(2)_L$ and $SU(3)_C$ gauge groups, respectively. These mass terms are assumed to be equal at the unification scale, leading to $M_1 = \frac{5}{3}M_2 \tan^2 \theta_W$ at the electroweak scale [29]. In the MSSM, the masses and the interactions of the gauginos and of the sparticles are entirely described [30] once the five parameters $\tan \beta$ (the ratio of the vacuum expectation values of the two higgs doublets), $M \equiv M_2$

(the gaugino mass parameter), μ (the higgsino mixing parameter), m_0 (the sparticle mass parameter) and A (the trilinear coupling in the Higgs sector) are fixed.

The parameters M and μ , together with $\tan\beta$, determine the field contents of the charginos as a mixing of gauginos and higgsinos. Charginos are produced in the s -channel by Z/γ exchange and in the t -channel by $\tilde{\nu}$ exchange. The interference between s -channel and t -channel can be either constructive or destructive, depending on the field contents of the chargino, *i.e.* on the amplitudes of its gaugino and higgsino components, and on the sneutrino mass. Gauginos couple to the sneutrino while higgsinos do not. If the chargino has a large higgsino component the effect of the interference is very small, and so is the dependence of the cross section on the sneutrino mass. On the other hand, if the chargino has a large gaugino component, the cross section shows a large dependence on $M_{\tilde{\nu}}$ for small sneutrino mass. For large sneutrino mass, $M_{\tilde{\nu}} > 200$ GeV, the chargino production cross section is independent of $M_{\tilde{\nu}}$ and only depends on the field contents of the chargino: in particular, it is minimum (maximum) for purely higgsino (gaugino) like chargino.

In Figure 4 we show the excluded region in the chargino and neutralino mass plane with $M_{\tilde{\nu}} > 200$ GeV and $M_{\tilde{\chi}^\pm} < M_{\tilde{\chi}_2^0}$. This case, with a higgsino-like chargino, gives the minimum production cross section. For instance if $M_{\tilde{\chi}_1^0} = 40$ GeV we exclude at 95% C.L. charginos with masses smaller than 65 GeV.

We take into account the possibility that $\tilde{\chi}_2^0$ is lighter than the chargino. In this case the decay topology can be complicated by a cascade decay: $\tilde{\chi}^\pm \rightarrow W^* \tilde{\chi}_2^0 \rightarrow f\bar{f}' Z^* \tilde{\chi}_1^0 \rightarrow f\bar{f}' f\bar{f} \tilde{\chi}_1^0$. Evaluating the efficiencies for this decay channel for different masses of $\tilde{\chi}^\pm$, $\tilde{\chi}_2^0$ and $\tilde{\chi}_1^0$ we observe a slight reduction of the efficiency depending on the masses of $\tilde{\chi}^\pm$, $\tilde{\chi}_2^0$ and $\tilde{\chi}_1^0$. To be conservative we take the highest reduction (about 35%) to evaluate the efficiency for this particular decay. In Figure 5 we show the excluded region at 95% C.L. in the $M - \mu$ plane of the MSSM resulting from the combined search for charginos and neutralinos for different values of $\tan\beta$ and of the sparticle mass parameter, m_0 . Even in the case of a light sneutrino, when the decays into $l\tilde{\nu}^*$ ($\tau\tilde{\nu}^*$ if the chargino is higgsino-like) are dominant, we have good sensitivity. This latter case is shown in Figure 5a–b where the parameter m_0 is equal to 30 GeV and where the slepton masses, for $M < 200$ GeV, are of the order of M_W . The small difference in the excluded region for low slepton masses, with respect to high slepton masses shown in Figure 5c–d, in addition to the enhancement of the leptonic branching ratios, is due to the enhancement of the selectron mediated t -channel production of neutralinos. The region inside the dotted line has already been excluded by a previous search performed with LEP I data [6].

The expected cross section for sleptons, with mass of about 50 GeV, is rather low (~ 0.5 pb) except for selectrons where it is enhanced by the t -channel contribution. We set limits only on the mass of the lightest selectron ($M_{\tilde{e}_R}$) and in Figure 6 we show the excluded region in the $M_{\tilde{e}_R} - M_{\tilde{\chi}_1^0}$ plane, obtained with $\tan\beta = 1.5$ and for any values of the parameters in the ranges $0 < M < 200$ GeV, $-200 < \mu < 200$ GeV and $0 < m_0 < 100$ GeV. We can not improve the LEP I exclusion in the MSSM, for smuon and stau, due to the low expected cross section.

According to MSSM predictions [31] limits can be obtained for the stop quark production only in the region of the parameter space, where $\cos\theta_{LR} \sim 1$, where the cross section is maximum. In Figure 7 we show the region excluded with this analysis in the case $\cos\theta_{LR} = 1$, as well as the region excluded at LEP I [7] up to $\sqrt{s} = 95$ GeV. Lower limits on the stop quark mass, obtained at LEP I [7], cannot be improved if we consider the minimum expected cross section.

9 Conclusions

A search for charginos, neutralinos, sleptons and stop quarks has been performed with data collected at the 130–140 GeV centre of mass energy run. We did not observe any candidate events and we considerably improve the exclusions obtained at LEP I.

Acknowledgments

We wish to express our gratitude to the CERN accelerator divisions for the excellent performance of the LEP machine. We acknowledge the contributions of all the engineers and technicians who have participated in the construction and maintenance of this experiment. Those of us who are not from member states thank CERN for its hospitality and help.

References

- [1] S.L. Glashow, Nucl. Phys. **22** (1961) 579;
S. Weinberg, Phys. Rev. Lett. **19** (1967) 1264;
A. Salam, Elementary Particle Theory, Ed. N. Svartholm, Stockholm, Almqvist and Wiksell (1968) 367.
- [2] Y.A. Goldfand and E.P. Likhtman, JETP Lett. **13** (1971) 323;
D.V. Volkov and V.P. Akulov, Phys. Lett. **B 46** (1973) 109;
J. Wess and B. Zumino, Nucl. Phys. **B 70** (1974) 39;
P. Fayet and S. Ferrara, Phys. Rep. **32** (1977) 249;
A. Salam and J. Strathdee, Fortschr. Phys. **26** (1978) 57.
- [3] S. Abachi *et al.*, Phys. Rev. Lett. **74** (1995) 2632;
F. Abe *et al.*, Phys. Rev. Lett. **74** (1995) 2626.
- [4] A. Bouquet *et al.*, Nucl. Phys. **B 262** (1985) 299;
J. Ellis and S. Rudaz, Phys. Lett. **B 128** (1983) 248.
- [5] ALEPH Collab., D. Decamp *et al.*, Phys. Rep. **216** (1992) 253;
DELPHI Collab., P. Abreu *et al.*, Phys. Lett. **B 247** (1990) 157;
L3 Collab., B. Adeva *et al.*, Phys. Lett. **B 233** (1989) 530;
OPAL Collab., M.Z. Akrawy *et al.*, Phys. Lett. **B 248** (1990) 211;
Particle Data Group, Phys. Rev. **D 50** (1994) 1791 and references therein.
- [6] L3 Collab., M. Acciarri *et al.*, Phys. Lett. **B 350** (1995) 109.
- [7] OPAL Collab., R. Akers *et al.*, Phys. Lett. **B 337** (1994) 207.
- [8] D0 Collab., contributed paper No. 434, EPS HEP Conference, August 1995;
CDF Collab., contributed paper No. 769, EPS HEP Conference, August 1995.
- [9] L3 Collab., B. Adeva *et al.*, Nucl. Inst. Meth. **A 289** (1990) 35.
- [10] M. Acciarri *et al.*, Nucl. Inst. Meth. **A 351** (1994) 300.
- [11] M. Chemarin *et al.*, Nucl. Inst. Meth. **A 349** (1994) 345.
- [12] A. Adam *et al.*, “The Forward Muon Detector of L3”, to be published in Nucl. Inst. Meth.
- [13] M. Merk, Proceedings of the XXIXth Rencontre de Moriond, Meribel les Allues, France – March 12–19, 1994, p. 93, ed. J. Tran Thanh Van.
- [14] T. Sjöstrand, Comp. Phys. Comm. **82** (1994) 74.
- [15] J. H. Field, Phys. Lett. **B 323** (1994) 432;
J. H. Field and T. Riemann, Preprints UGVA–DPNC 1995/6–166 and DESY 95–100,
to be published in Comp. Phys. Comm.
- [16] The KORALZ version 4.01 is used.
S. Jadach, B. F. L. Ward and Z. Wąs, Comp. Phys. Comm. **79** (1994) 503.

- [17] Monte Carlo program KORALW 1.02.
M. Skrzypek, S. Jadach, W. Placzek and Z. Was, CERN preprint CERN-TH/95-205, to appear in *Comp. Phys. Comm.* .
- [18] S. Katsanevas and S. Melacrinios, "SUSYGEN", to be published in the proceedings of the "Workshop on Physics at LEP2", CERN, 1995.
- [19] C. Dionisi, K. Fujii, S. Giagu and T. Tsukamoto, "DFGT: a chargino Montecarlo generator which deals with spin correlation", to be published in the proceedings of the "Workshop on Physics at LEP2" .
- [20] A. Sopczak, to be published in the proceedings of the Workshop on Physics at LEP2 .
- [21] The L3 detector simulation is based on GEANT Version 3.15.
R. Brun *et al.*, "GEANT 3", CERN-DD/EE/84-1 (Revised), 1987.
The GHEISHA program (H. Fesefeldt, RWTH Aachen Report PITHA 85/02 (1985)) is used to simulate hadronic interactions.
- [22] G. Carlino, X. Chereau, G. Coignet and S. Rosier, L3 Internal Note 1897, Dec. 1995¹⁾;
F. Di Lodovico and M. Felcini, L3 Internal Note 1886, Dec. 1995¹⁾;
C. Dionisi, S. Giagu and C. Luci, L3 Internal Note 1888, Dec. 1995¹⁾;
V. Innocente, L. Lista and S. Mele, L3 Internal Note 1875, Dec. 1995¹⁾.
- [23] O. Adriani, A. Favara, M. Pieri and E. Pistolesi, L3 Internal Note 1896, Dec. 1995¹⁾.
- [24] S. Banerjee, S. Bhattacharya, G. Majumder, L3 Internal Note 1885, Dec. 1995¹⁾.
- [25] H. Nowak and A. Sopczak, L3 Internal Note 1887, Dec. 1995¹⁾.
- [26] T. Sjöstrand, *Comp. Phys. Comm.* **39** (1986) 347;
T. Sjöstrand and M. Bengtsson, *Comp. Phys. Comm.* **43** (1987) 367.
- [27] J.F. Grivaz, F. Le Diberder, preprint LAL-92-37, June 1992, LAL, IN2P3-CNRS, France.
- [28] J. Ellis *et al.*, *Mod. Phys. Lett. A* **1** (1986) 57;
R. Barbieri and G.F. Giudice, *Nucl. Phys. B* **306** (1988) 63;
Z. Kunszt and F. Zwirner, CERN-TH.6150/91, ETH-TH/91-7, Dec. 91.
- [29] For reviews, see H. Nilles, *Phys. Rep.* **110** (1984) 1;
H. E. Haber and G. Kane, *Phys. Rep.* **117** (1985) 75;
R. Barbieri, *Riv. Nuovo Cimento* **11**, No. 4 (1988) 75.
- [30] A. Bartl, H. Fraas, W. Majerotto, and B. Mösslacher, *Z. Phys. C* **55** (1992) 257, and references therein;
S. Ambrosanio and B. Mele, *Phys. Rev. D* **52** (1995) 3900;
A. Bartl, H. Fraas and W. Majerotto, *Z. Phys. C* **34** (1987) 411;
S. Ambrosanio and B. Mele, "Neutralino Decays in the Minimal Supersymmetric Standard Model", Preprint ROME1-1095/95, hep-ph/9508237, August 1995, to appear in *Phys. Rev. D*.
- [31] A. Bartl *et al.*, private communications.

¹⁾These L3 Internal Notes are freely available on request from: The L3 secretariat, CERN, CH-1211 Geneva 23, Switzerland. Internet: <http://hpl3sn02.cern.ch/l3pubanddoc.html>

The L3 Collaboration:

M.Acciarri,²⁹ A.Adam,⁴⁸ O.Adriani,¹⁸ M.Aguilar-Benitez,²⁸ S.Ahlen,¹² B.Alpat,³⁶ J.Alcaraz,²⁸ G.Alemanni,²⁴ J.Allaby,¹⁹ A.Aloisio,³¹ G.Alverson,¹³ M.G.Alvigi,³¹ G.Ambrosi,³⁶ H.Anderhub,⁵¹ V.P.Andreev,⁴⁰ T.Angelescu,¹⁴ D.Antreasyan,¹⁰ A.Arefev,³⁰ T.Azmoon,³ T.Aziz,¹¹ P.Bagnaia,³⁹ L.Baksay,⁴⁶ R.C.Ball,³ S.Banerjee,¹¹ K.Banicz,⁴⁸ R.Barillere,¹⁹ L.Barone,³⁹ P.Bartalini,³⁶ A.Baschirotto,²⁹ M.Basile,¹⁰ R.Battiston,³⁶ A.Bay,²⁴ F.Becattini,¹⁸ U.Becker,¹⁷ F.Behner,⁵¹ J.Berdugo,²⁸ P.Berges,¹⁷ B.Bertucci,¹⁹ B.L.Betev,⁵¹ M.Biasini,¹⁹ A.Biland,⁵¹ G.M.Bilei,³⁶ J.J.Blaising,¹⁹ S.C.Blyth,³⁷ G.J.Bobbink,² R.Bock,¹ A.Böhm,¹ B.Borgia,³⁹ A.Boucham,⁴ D.Bourilkov,⁵¹ M.Bourquin,²¹ E.Brambilla,¹⁷ J.G.Branson,⁴² V.Brigljevic,⁵¹ I.C.Brock,³⁷ A.Buijs,⁴⁷ A.Bujak,⁴⁸ J.D.Burger,¹⁷ W.J.Burger,²¹ J.Busenitz,⁴⁶ A.Buytenhuijs,³³ X.D.Cai,²⁰ M.Campanelli,⁵¹ M.Capell,⁷ G.Cara Romeo,⁰ M.Carria,³⁶ G.Carlini,⁴ A.M.Cartacci,¹⁸ J.Casaus,²⁸ G.Castellini,¹⁸ R.Castello,²⁹ F.Cavallari,³⁹ N.Cavallo,³¹ C.Cecchi,²¹ M.Cerrada,²⁸ F.Cesaroni,²⁵ M.Chamizo,²⁸ A.Chan,⁵³ Y.H.Chang,⁵³ U.K.Chaturvedi,²⁰ M.Chemarin,²⁷ A.Chen,⁵³ C.Chen,⁸ G.Chen,⁸ G.M.Chen,⁸ H.F.Chen,²² H.S.Chen,⁸ X.Chereau,⁴ G.Chiefari,³¹ C.Y.Chien,⁵ M.T.Choi,⁴⁵ L.Cifarelli,⁴¹ F.Cindolo,¹⁰ C.Civinini,¹⁸ I.Clare,¹⁷ R.Clare,¹⁷ H.O.Cohn,³⁴ G.Coignet,⁴ A.P.Colijn,² N.Colino,²⁸ V.Commicchau,¹ S.Costantini,³⁹ F.Cotorobai,⁴ B.de la Cruz,²⁸ T.S.Dai,¹⁷ R.D'Alessandro,¹⁸ R.de Asmundis,³¹ H.De Boeck,³³ A.Degré,⁴ K.Deiters,⁴⁹ P.Denes,³⁸ F.DeNotaristefani,³⁹ D.DiBitonto,⁴⁶ M.Diemoz,³⁹ D.van Dierendonck,² F.Di Lodovico,⁵¹ C.Dionisi,³⁹ M.Dittmar,⁵¹ A.Dominguez,⁴² A.Doria,³¹ I.Dorne,⁴ M.T.Dova,^{20,†} E.Drago,³¹ D.Duchesneau,⁴ P.Duinker,² I.Duran,⁴³ S.Dutta,¹¹ S.Easo,³⁶ Yu.Efremenko,³⁴ H.El Mamouni,²⁷ A.Engler,³⁷ F.J.Eppling,¹⁷ F.C.Erné,² J.P.Ernenwein,²⁷ P.Extermann,²¹ M.Fabre,⁴⁹ R.Faccini,³⁹ S.Falciano,³⁹ A.Favara,¹⁸ J.Fay,²⁷ M.Felcini,⁵¹ T.Ferguson,³⁷ D.Fernandez,²⁸ F.Ferroni,³⁹ H.Fesefeldt,¹ E.Fiandrini,³⁶ J.H.Field,²¹ F.Filthaut,³⁷ P.H.Fisher,¹⁷ G.Forconi,¹⁷ L.Fredj,²¹ K.Freudenreich,⁵¹ Yu.Galaktionov,^{30,17} S.N.Ganguli,¹¹ S.S.Gau,¹³ S.Gentile,³⁹ J.Gerald,⁵ N.Gheordanescu,¹⁴ S.Giagu,³⁹ S.Goldfarb,²⁴ J.Goldstein,¹² Z.F.Gong,²² A.Gougas,⁵ G.Gratta,³⁵ M.W.Gruenewald,⁹ V.K.Gupta,³⁸ A.Gurtu,¹¹ L.J.Gutay,⁴⁸ K.Hangarter,¹ B.Hartmann,¹ A.Hasan,³² J.T.He,⁸ T.Hebbeker,⁹ A.Hervé,¹⁹ W.C.van Hoek,³³ H.Hofer,⁵¹ H.Hoorani,²¹ S.R.Hou,⁵³ G.Hu,²⁰ M.M.Ilyas,²⁰ V.Innocente,¹⁹ H.Janssen,⁴ B.N.Jin,⁸ L.W.Jones,³ P.de Jong,¹⁷ I.Josa-Mutuberria,²⁸ A.Kasser,²⁴ R.A.Khan,²⁰ Yu.Kamyshkov,³⁴ P.Kapinos,⁵⁰ J.S.Kapustinsky,²⁶ Y.Karyotakis,⁴ M.Kaur,^{20,◇} M.N.Kienzle-Focacci,²¹ D.Kim,⁵ J.K.Kim,⁴⁵ S.C.Kim,⁴⁵ Y.G.Kim,⁴⁵ W.W.Kinnison,²⁶ A.Kirkby,³⁵ D.Kirkby,³⁵ J.Kirkby,¹⁹ W.Kittel,³³ A.Klimentov,^{17,30} A.C.König,³³ A.Königter,¹ I.Korolko,³⁰ V.Koutsenko,^{17,30} A.Koulbardi,⁴⁰ R.W.Kraemer,³⁷ T.Kramer,¹⁷ W.Krenz,¹ H.Kuijten,³³ A.Kunin,^{17,30} P.Ladron de Guevara,²⁸ G.Landi,¹⁸ C.Lapoint,¹⁷ K.Lassila-Perini,⁵¹ M.Lebeau,¹⁹ A.Lebedev,¹⁷ P.Lebrun,²⁷ P.Lecomte,⁵¹ P.Lecoq,¹⁹ P.Le Coultre,⁵¹ J.S.Lee,⁴⁵ K.Y.Lee,⁴⁵ J.M.Le Goff,¹⁹ R.Leiste,⁵⁰ M.Lenti,¹⁸ E.Leonardi,³⁹ P.Levtchenko,⁴⁰ C.Li,²² E.Lieb,⁵⁰ W.T.Lin,⁵³ F.L.Linde,^{2,19} B.Lindemann,¹ L.Lista,³¹ Z.A.Liu,⁸ W.Lohmann,⁵⁰ E.Longo,³⁹ W.Lu,³⁵ Y.S.Lu,⁸ K.Lübelsmeyer,¹ C.Luci,³⁹ D.Luckey,¹⁷ L.Ludovici,³⁹ L.Luminari,³⁹ W.Lustermann,⁴⁹ W.G.Ma,²² A.Macchiolo,¹⁸ M.Maity,¹¹ G.Majumder,¹¹ L.Malgeri,³⁹ A.Malinin,³⁰ C.Maña,²⁸ S.Mangla,¹¹ P.Marchesini,⁵¹ A.Marin,² J.P.Martin,²⁷ F.Marzano,³⁹ G.G.G.Massarò,² K.Mazumdar,¹¹ D.McNally,¹⁹ R.R.McNeil,⁷ S.Mele,³¹ L.Merola,³¹ M.Meschini,¹⁸ W.J.Metzger,³³ M.von der Mey,¹ Y.Mi,²⁴ A.Mihul,¹⁴ A.J.W.van Mil,³³ G.Mirabelli,³⁹ J.Mnich,¹⁹ M.Möller,¹ B.Monteoloni,¹⁸ R.Moore,³ S.Morganti,³⁹ R.Mount,³⁵ S.Müller,¹ F.Muheim,²¹ E.Nagy,¹⁵ S.Nahn,¹⁷ M.Napolitano,³¹ F.Nessi-Tedaldi,⁵¹ H.Newman,³⁵ A.Nippe,¹ H.Nowak,⁵⁰ G.Organtini,³⁹ R.Ostonen,²³ D.Pandoulas,¹ S.Paoletti,³⁹ P.Paolucci,³¹ H.K.Park,³⁷ G.Pascale,³⁹ G.Passaleva,¹⁸ S.Patricelli,³¹ T.Paul,³⁶ M.Pauluzzi,³⁶ C.Paus,¹ F.Pauss,⁵¹ D.Peach,¹⁹ Y.J.Pei,¹ S.Pensotti,²⁹ D.Perret-Gallix,⁴ S.Petrak,⁹ A.Pevsner,⁵ D.Piccolo,³¹ M.Pieri,¹⁸ J.C.Pinto,³⁷ P.A.Piroué,³⁸ E.Pistolesi,¹⁸ V.Plyaskin,³⁰ M.Pohl,⁵¹ V.Pojidaev,^{30,18} H.Postema,¹⁷ N.Produit,²¹ R.Raghavan,¹¹ G.Rahal-Callot,⁵¹ P.G.Rancoita,²⁹ M.Rattaggi,²⁹ G.Raven,⁴² P.Razis,³² K.Read,³⁴ M.Redaeli,²⁹ D.Ren,⁵¹ M.Rescigno,³⁹ S.Reucroft,¹³ A.Ricker,¹ S.Riemann,⁵⁰ B.C.Riemers,⁴⁸ K.Riles,³ S.Ro,⁴⁵ A.ROBOHM,⁵¹ J.Rodin,¹⁷ F.J.Rodriguez,²⁸ B.P.Roe,³ S.Röhner,¹ L.Romero,²⁸ S.Rosier-Lees,⁴ Ph.Rosselet,²⁴ W.van Rossum,⁴⁷ S.Roth,¹ J.A.Rubio,¹⁹ H.Rykaczewski,⁵¹ J.Salicio,¹⁹ E.Sanchez,²⁸ A.Santocchia,³⁶ M.E.Sarakinos,²³ S.Sarkar,¹¹ M.Sassowsky,¹ C.Schäfer,¹ V.Schegelsky,⁴⁰ S.Schmidt-Kaerst,¹ D.Schmitz,¹ P.Schmitz,¹ M.Schneegans,⁴ B.Schoeneich,⁵⁰ N.Scholz,⁵¹ H.Schopper,⁵² D.J.Schotanus,³³ R.Schulte,¹ K.Schultze,¹ J.Schwenke,¹ G.Schwering,¹ C.Sciacca,³¹ D.Sciarrino,²¹ J.C.Sens,⁵³ L.Servoli,³⁶ S.Shevchenko,³⁵ N.Shivarov,⁴⁴ V.Shoutko,³⁰ J.Shukla,²⁶ E.Shumilov,³⁰ T.Siedenburger,¹ D.Son,⁴⁵ A.Sopczak,⁵⁰ B.Smith,¹⁷ P.Spillantini,¹⁸ M.Steuer,¹⁷ D.P.Stickland,³⁸ F.Sticozzi,¹⁷ H.Stone,³⁸ B.Stoyanov,⁴⁴ A.Straessner,¹ K.Strauch,¹⁶ K.Sudhakar,¹¹ G.Sultanov,²⁰ L.Z.Sun,²² G.F.Susinno,²¹ H.Suter,⁵¹ J.D.Swain,²⁰ X.W.Tang,⁸ L.Tauscher,⁶ L.Taylor,¹³ Samuel C.C.Ting,¹⁷ S.M.Ting,¹⁷ O.Toker,³⁶ F.Tonisch,⁵⁰ M.Tonutti,¹ S.C.Tonwar,¹¹ J.Tóth,¹⁵ A.Tsaregorodtsev,⁴⁰ C.Tully,³⁸ H.Tuchscherer,⁴⁶ K.L.Tung,⁸ J.Ulbricht,⁵¹ U.Uwer,¹⁹ E.Valente,³⁹ R.T.Van de Walle,³³ I.Vetlitsky,³⁰ G.Viertel,⁵¹ M.Vivargent,⁴ R.Völkert,⁵⁰ H.Vogel,³⁷ H.Vogt,⁵⁰ I.Vorobiev,³⁰ A.A.Vorobyov,⁴⁰ An.A.Vorobyov,⁴⁰ A.Vorvolakos,³² M.Wadhwa,⁶ W.Wallraff,¹ J.C.Wang,¹⁷ X.L.Wang,²² Y.F.Wang,¹⁷ Z.M.Wang,²² A.Weber,¹ F.Wittgenstein,¹⁹ S.X.Wu,²⁰ S.Wynhoff,¹ J.Xu,¹² Z.Z.Xu,²² B.Z.Yang,²² C.G.Yang,⁸ X.Y.Yao,⁸ J.B.Ye,²² S.C.Yeh,⁵³ J.M.You,³⁷ C.Zaccardelli,³⁵ An.Zalite,⁴⁰ P.Zemp,⁵¹ J.Y.Zeng,⁸ Y.Zeng,¹ Z.Zhang,⁸ Z.P.Zhang,²² B.Zhou,¹² G.J.Zhou,⁸ Y.Zhou,³ G.Y.Zhu,⁸ R.Y.Zhu,³⁵ A.Zichichi,^{10,19,20}

- 1 I. Physikalisches Institut, RWTH, D-52056 Aachen, FRG[§]
 - III. Physikalisches Institut, RWTH, D-52056 Aachen, FRG[§]
 - 2 National Institute for High Energy Physics, NIKHEF, and University of Amsterdam, NL-1009 DB Amsterdam, The Netherlands
 - 3 University of Michigan, Ann Arbor, MI 48109, USA
 - 4 Laboratoire d'Annecy-le-Vieux de Physique des Particules, LAPP,IN2P3-CNRS, BP 110, F-74941 Annecy-le-Vieux CEDEX, France
 - 5 Johns Hopkins University, Baltimore, MD 21218, USA
 - 6 Institute of Physics, University of Basel, CH-4056 Basel, Switzerland
 - 7 Louisiana State University, Baton Rouge, LA 70803, USA
 - 8 Institute of High Energy Physics, IHEP, 100039 Beijing, China
 - 9 Humboldt University, D-10099 Berlin, FRG[§]
 - 10 INFN-Sezione di Bologna, I-40126 Bologna, Italy
 - 11 Tata Institute of Fundamental Research, Bombay 400 005, India
 - 12 Boston University, Boston, MA 02215, USA
 - 13 Northeastern University, Boston, MA 02115, USA
 - 14 Institute of Atomic Physics and University of Bucharest, R-76900 Bucharest, Romania
 - 15 Central Research Institute for Physics of the Hungarian Academy of Sciences, H-1525 Budapest 114, Hungary[‡]
 - 16 Harvard University, Cambridge, MA 02139, USA
 - 17 Massachusetts Institute of Technology, Cambridge, MA 02139, USA
 - 18 INFN Sezione di Firenze and University of Florence, I-50125 Florence, Italy
 - 19 European Laboratory for Particle Physics, CERN, CH-1211 Geneva 23, Switzerland
 - 20 World Laboratory, FBLJA Project, CH-1211 Geneva 23, Switzerland
 - 21 University of Geneva, CH-1211 Geneva 4, Switzerland
 - 22 Chinese University of Science and Technology, USTC, Hefei, Anhui 230 029, China
 - 23 SEFT, Research Institute for High Energy Physics, P.O. Box 9, SF-00014 Helsinki, Finland
 - 24 University of Lausanne, CH-1015 Lausanne, Switzerland
 - 25 INFN-Sezione di Lecce and Università Degli Studi di Lecce, I-73100 Lecce, Italy
 - 26 Los Alamos National Laboratory, Los Alamos, NM 87544, USA
 - 27 Institut de Physique Nucléaire de Lyon, IN2P3-CNRS, Université Claude Bernard, F-69622 Villeurbanne, France
 - 28 Centro de Investigaciones Energeticas, Medioambientales y Tecnológicas, CIEMAT, E-28040 Madrid, Spain[‡]
 - 29 INFN-Sezione di Milano, I-20133 Milan, Italy
 - 30 Institute of Theoretical and Experimental Physics, ITEP, Moscow, Russia
 - 31 INFN-Sezione di Napoli and University of Naples, I-80125 Naples, Italy
 - 32 Department of Natural Sciences, University of Cyprus, Nicosia, Cyprus
 - 33 University of Nymegen and NIKHEF, NL-6525 ED Nymegen, The Netherlands
 - 34 Oak Ridge National Laboratory, Oak Ridge, TN 37831, USA
 - 35 California Institute of Technology, Pasadena, CA 91125, USA
 - 36 INFN-Sezione di Perugia and Università Degli Studi di Perugia, I-06100 Perugia, Italy
 - 37 Carnegie Mellon University, Pittsburgh, PA 15213, USA
 - 38 Princeton University, Princeton, NJ 08544, USA
 - 39 INFN-Sezione di Roma and University of Rome, "La Sapienza", I-00185 Rome, Italy
 - 40 Nuclear Physics Institute, St. Petersburg, Russia
 - 41 University and INFN, Salerno, I-84100 Salerno, Italy
 - 42 University of California, San Diego, CA 92093, USA
 - 43 Dept. de Física de Partículas Elementales, Univ. de Santiago, E-15706 Santiago de Compostela, Spain
 - 44 Bulgarian Academy of Sciences, Central Laboratory of Mechatronics and Instrumentation, BU-1113 Sofia, Bulgaria
 - 45 Center for High Energy Physics, Korea Advanced Inst. of Sciences and Technology, 305-701 Taejon, Republic of Korea
 - 46 University of Alabama, Tuscaloosa, AL 35486, USA
 - 47 Utrecht University and NIKHEF, NL-3584 CB Utrecht, The Netherlands
 - 48 Purdue University, West Lafayette, IN 47907, USA
 - 49 Paul Scherrer Institut, PSI, CH-5232 Villigen, Switzerland
 - 50 DESY-Institut für Hochenergiephysik, D-15738 Zeuthen, FRG
 - 51 Eidgenössische Technische Hochschule, ETH Zürich, CH-8093 Zürich, Switzerland
 - 52 University of Hamburg, D-22761 Hamburg, FRG
 - 53 High Energy Physics Group, Taiwan, China
- [§] Supported by the German Bundesministerium für Bildung, Wissenschaft, Forschung und Technologie
[‡] Supported by the Hungarian OTKA fund under contract number T14459.
[‡] Supported also by the Comisión Interministerial de Ciencia y Tecnología
[‡] Also supported by CONICET and Universidad Nacional de La Plata, CC 67, 1900 La Plata, Argentina
[◇] Also supported by Panjab University, Chandigarh-160014, India

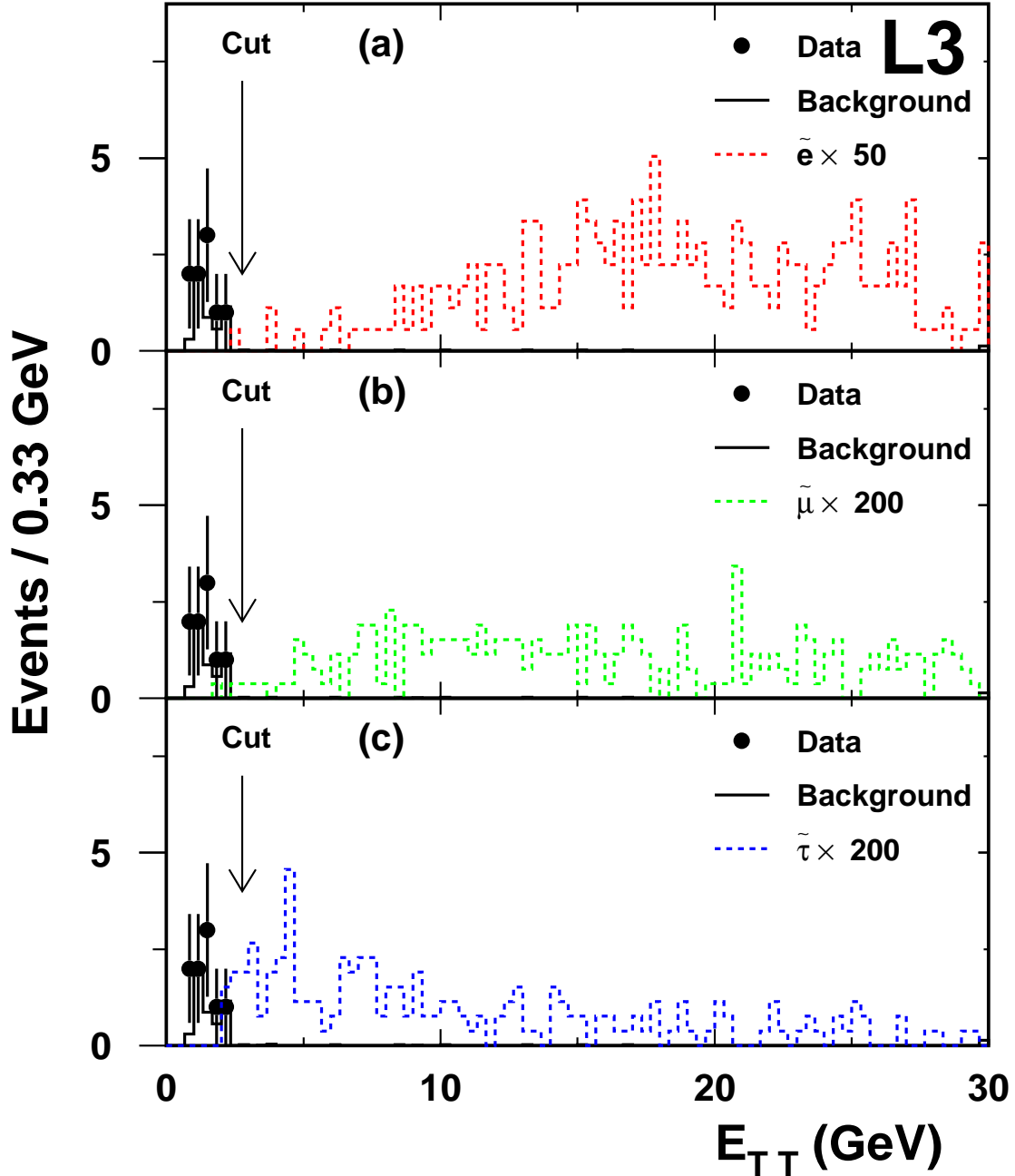


Figure 1: In (a) we show the distribution for data, expected background and the expected selectron signal when only the cut on the variable E_{TT} corresponding to the tau-tau selection is released in the final selection. In (b) we show the same distribution for smuons and in (c) for staus. The signal distributions, which are shown, are the ones obtained for $M_{slepton} = 60$ GeV and $M_{\tilde{\chi}_1^0} = 23$ GeV with the following values of the supersymmetric parameters: $M = 40$ GeV, $\mu = -200$ GeV, $\tan\beta = 1.5$, $m_0 = 50$ GeV and $A = 0$, for which the expected cross section for selectron is 0.8 pb and 0.4 pb at respectively 136 GeV and 130 GeV of centre of mass energy, while for smuons and staus is 0.14 pb and 0.08 pb at the same centre of mass energies as before.

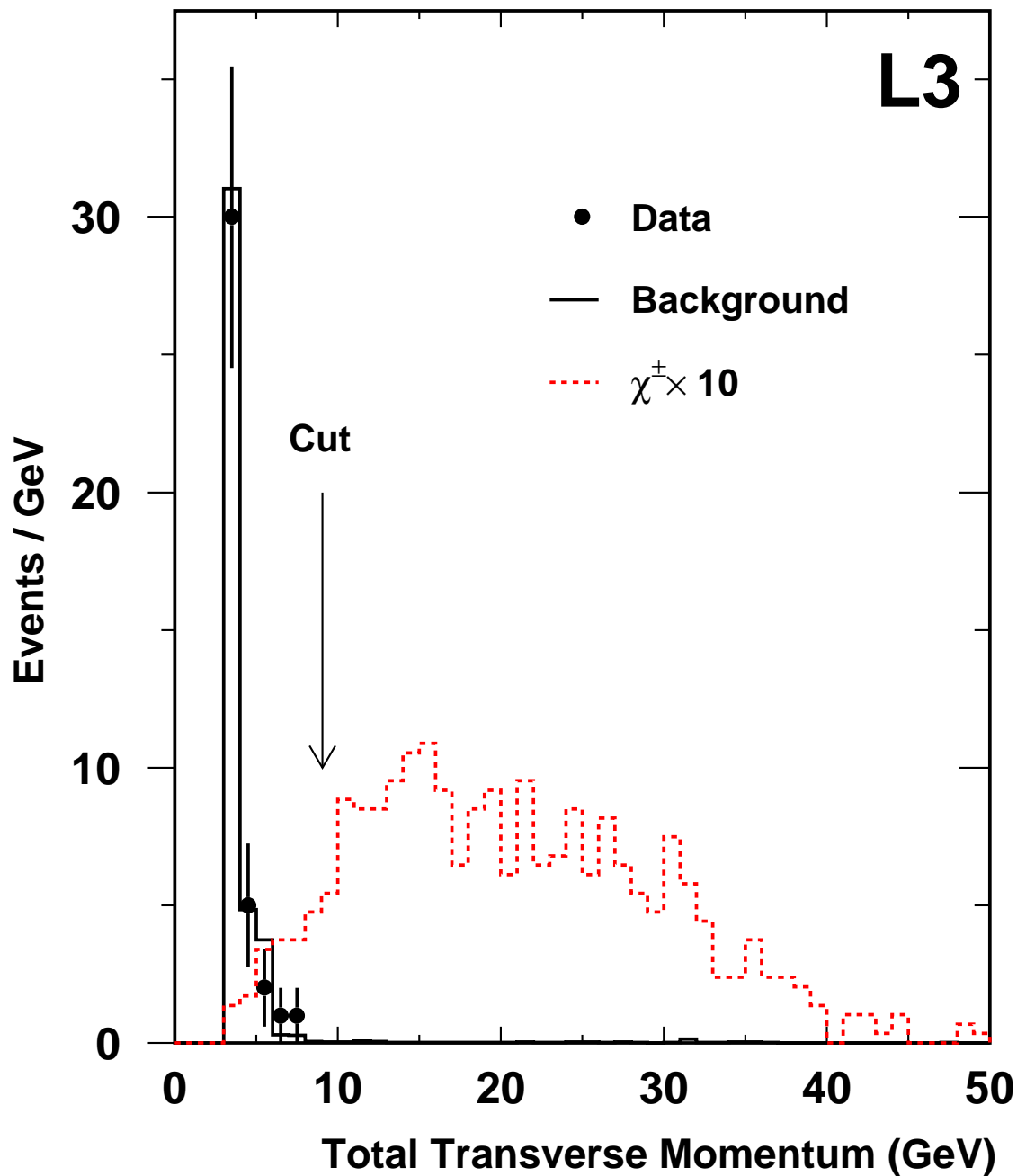


Figure 2: The distribution for data, expected background and charginos when only the cut on the total transverse missing momentum corresponding to the large multiplicity and large mass difference selection is released in the final selection. The signal distribution, which is shown, is the one obtained for $M_{\tilde{\chi}^\pm} = 60$ GeV and $M_{\tilde{\chi}_1^0} = 31$ GeV with the following values of the supersymmetric parameters: $M = 130$ GeV, $\mu = 145$ GeV, $\tan\beta = 1.5$, $m_0 = 100$ GeV and $A = 0$, for which the expected cross section is 7.1 pb and 7.2 pb at respectively 136 GeV and 130 GeV of centre of mass energy.

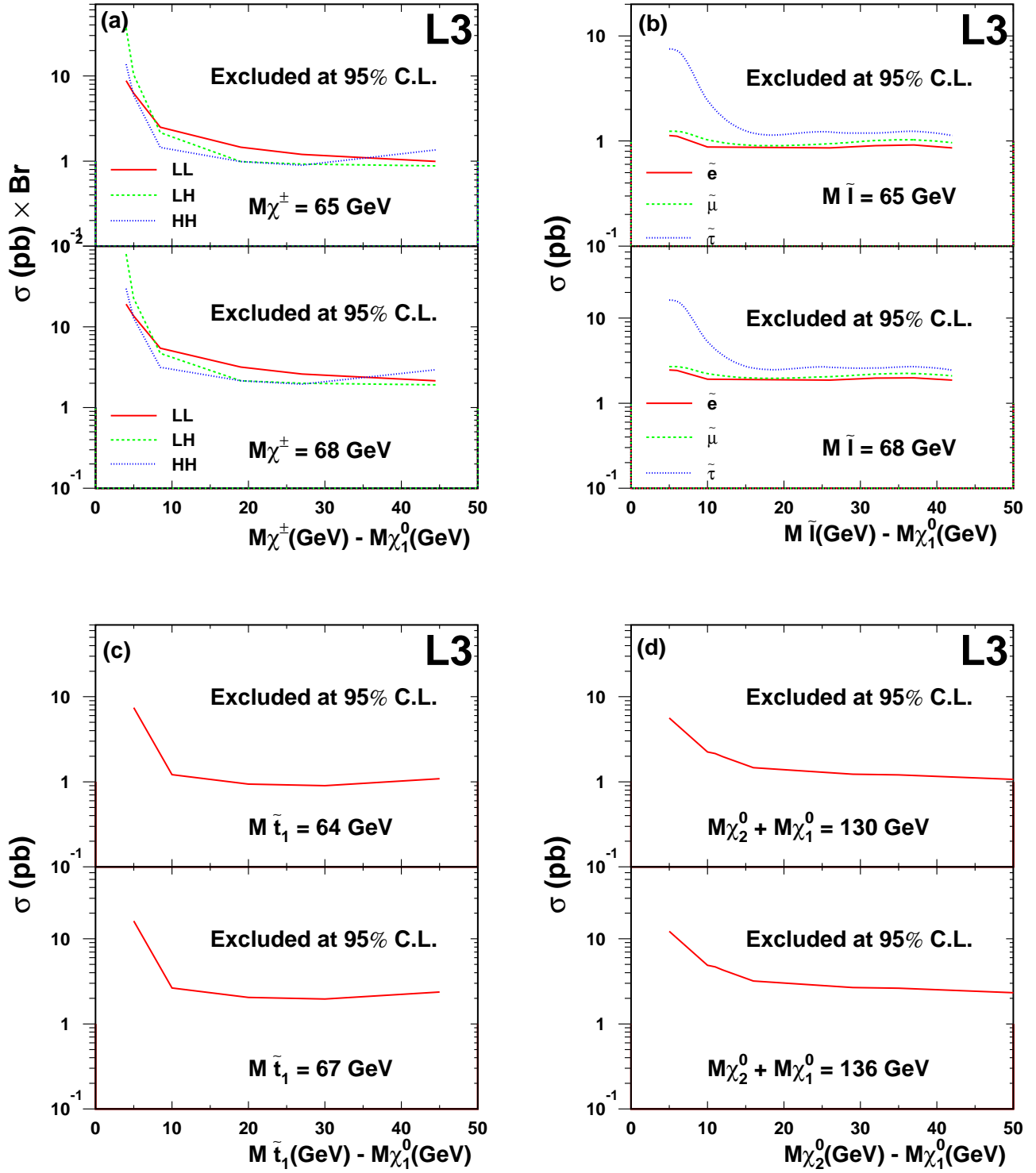


Figure 3: Upper limits on the production cross section for (a) charginos, (b) sleptons, (c) stop quarks and (d) neutralinos at the kinematic limit, at centre of mass energies of 130.3 and 136.3 GeV. In (a) the lines labelled LL, LH and HH show respectively the upper limit on the production cross section times the branching ratio into purely leptonic, semileptonic and purely hadronic charginos final states.

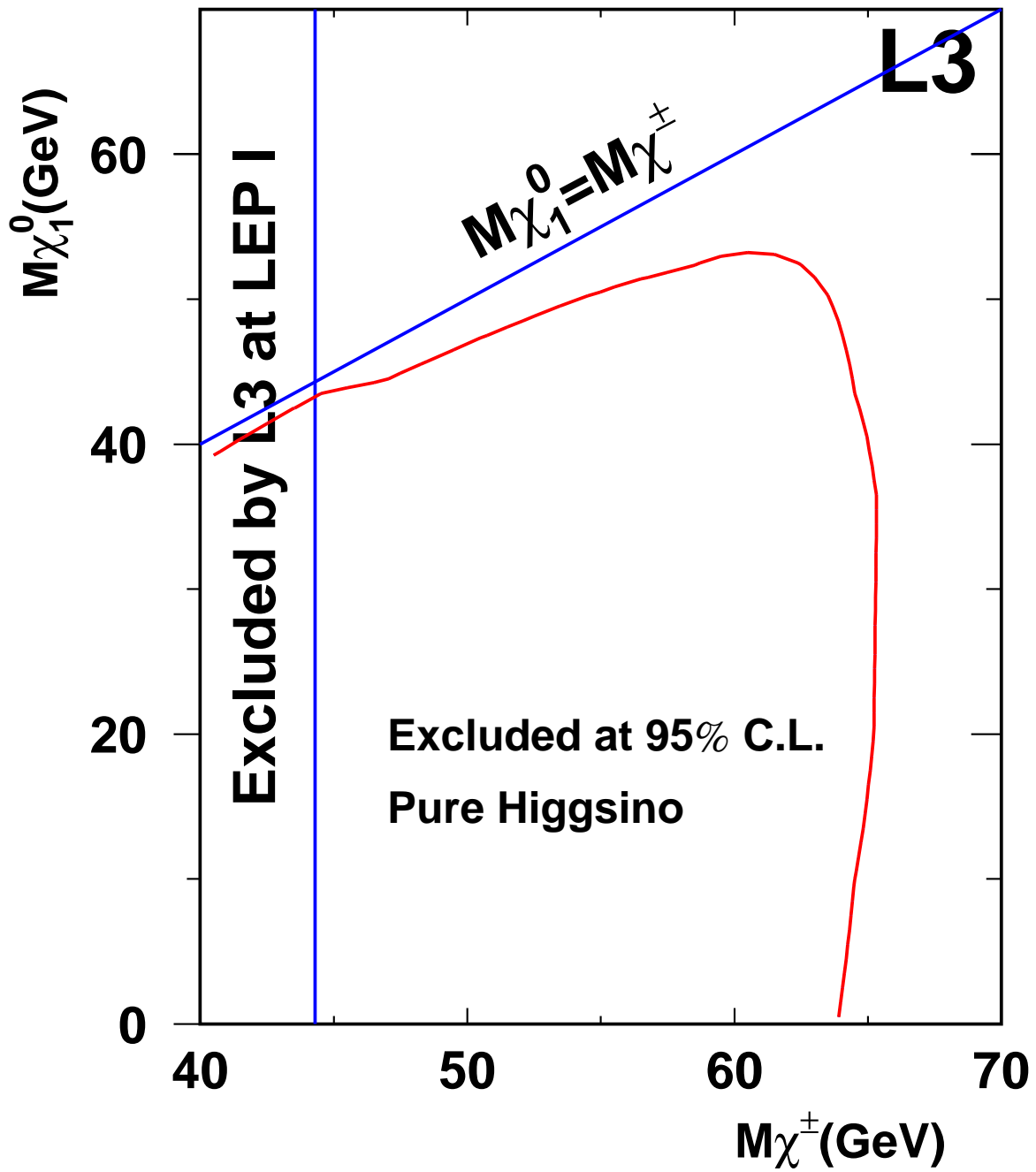


Figure 4: Excluded region in the chargino and neutralino mass plane, independent of the values of the MSSM parameters, for $M_{\tilde{\nu}} > 200$ GeV and $M_{\tilde{\chi}^\pm} < M_{\tilde{\chi}_2^0}$.

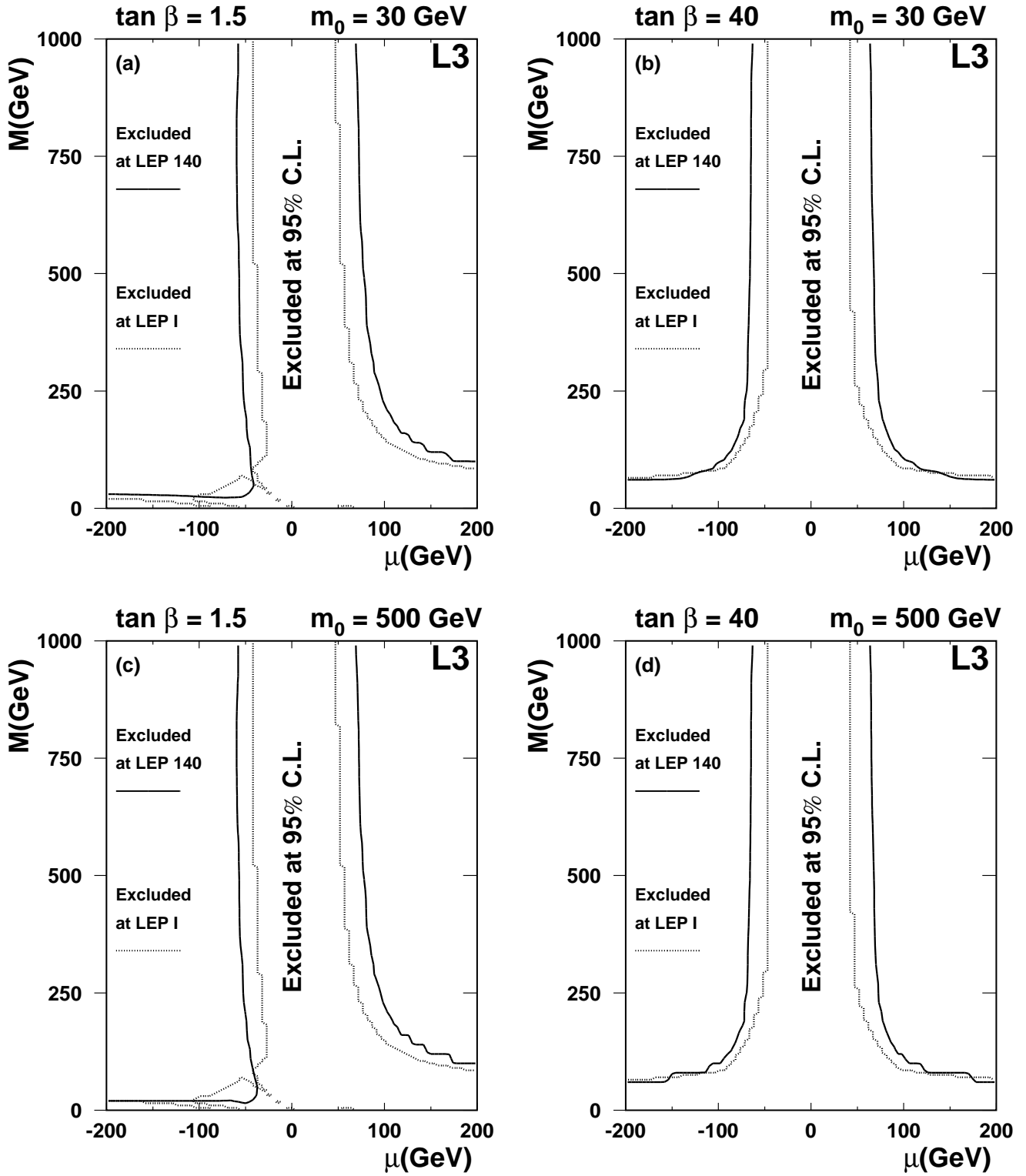


Figure 5: Excluded region, in the $M - \mu$ plane, for different values of $\tan \beta$ and of the sparticle mass parameter from the results of the combined search for charginos and neutralinos. For $M < 200$ GeV and for m_0 small the slepton masses are of the order of M_W , this implies a difference in the excluded region with respect to high values of m_0 . The excluded region at LEP I is also indicated with the dotted line.

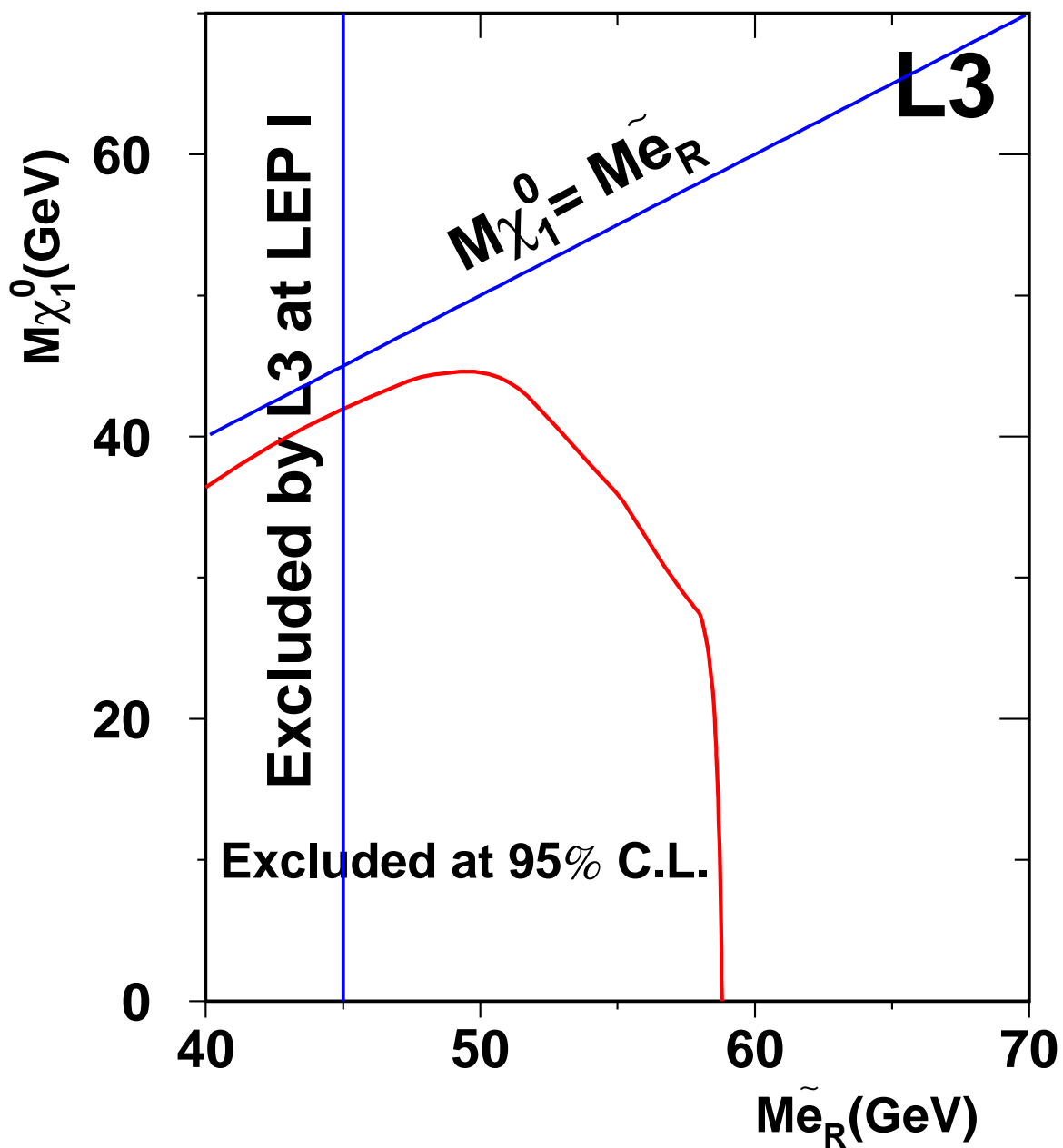


Figure 6: Excluded region, in the $M_{\tilde{e}_R} - M_{\tilde{\chi}_1^0}$ plane, with $\tan\beta = 1.5$ and for any values of the parameters in the ranges $0 < \tilde{M} < 200$ GeV, $-200 < \mu < 200$ GeV and $0 < m_0 < 100$ GeV.

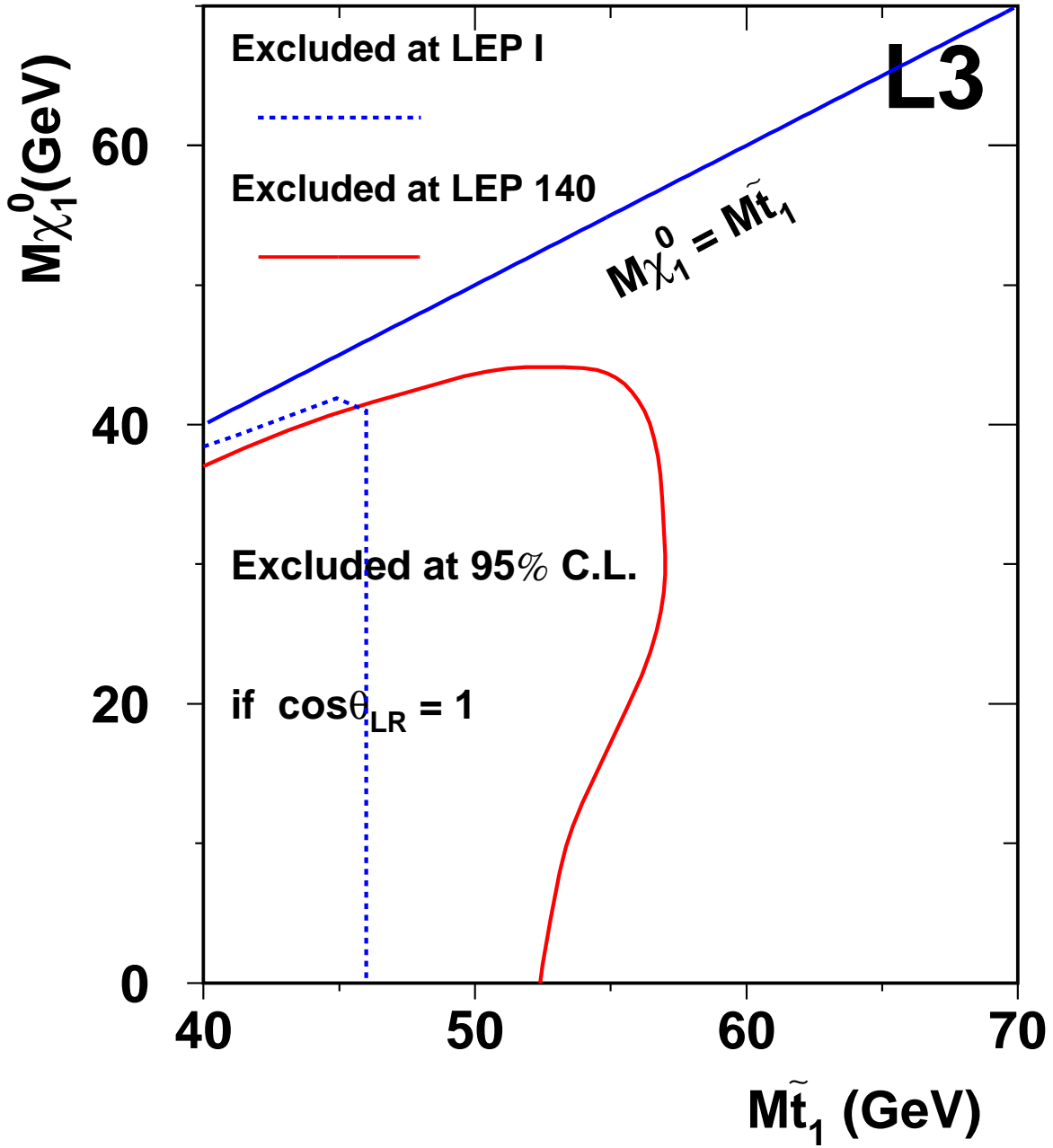


Figure 7: Excluded mass region as function of stop quark and neutralino masses for the choice $\cos\theta_{LR} = 1$. The region on the left of the dashed line has already been excluded at LEP I.